A VARIATIONAL APPROACH TO MODELING SLOW PROCESSES IN STOCHASTIC DYNAMICAL SYSTEMS

FRANK NOÉ

ABSTRACT. The slow processes of metastable stochastic dynamical systems are difficult to access by direct numerical simulation due the sampling problem. Here, we suggest an approach for modeling the slow parts of Markov processes by approximating the dominant eigenfunctions and eigenvalues of the propagator. To this end, a variational principle is derived that is based on the maximization of a Raleigh coefficient. It is shown that this Raleigh coefficient can be estimated from statistical observables that can be obtained from short distributed simulations starting from different parts of state space. The approach forms a basis for the development of adaptive and efficient computational algorithms for simulating and analyzing metastable Markov processes while avoiding the sampling problem. Since any stochastic process with finite memory can be transformed into a Markov process, the approach is applicable to a wide range of processes relevant for modeling complex real-world phenomena.

1. INTRODUCTION

In this article, we consider continuous-time Markov processes $\mathbf{z}_t \in \Omega$ living in a usually large state space Ω that is either continuous or discrete. The process $\mathbf{z}_t$ is considered to be sufficiently ergodic such that a unique stationary density (invariant measure) μ exists. Independent of the details of the dynamics (such as system size, potential, stochastic coupling, etc), there exists a family of linear propagators $\mathcal{P}(\tau)$ which evolve the probability density of states p_t as:

$$(1.1) \qquad\qquad p_\tau = \mathcal{P}(\tau)\, p_0$$

Continuous-time Markov processes are useful models of real-world processes in a variety of areas [39]. Examples include macroscopic phenomena including the evolution of financial and climate systems [20, 26], as well as microscopic dynamics such as the diffusion of cells in liquids [1], the diffusion of biomolecules within cells [36], the stochastic reaction dynamics of chemicals at surfaces [27], and the stochastic dynamics governing the structural dynamics of molecules [2]. Often, these dynamics are metastable, i.e. they consist of slow processes between sets of state space that have long lifetimes. In macromolecules, such slowly-exchanging sets are called conformations, hence the union of the slowest dynamical processes are there termed conformation dynamics [31, 33].

In practice, the slow dynamical processes are the ones which pose the greatest difficulties to direct numerical simulation as they require the longest simulation times. An extreme example is the atomistic simulation of solvated biomolecules which would require the propagation of a system with $10^4 - 10^6$ particles system for $10^7 - 10^{10}$ time-steps, a task that is intractable or hardly tractable even with special-purpose supercomputers [34]. However, the slowest processes are also the ones that are the most interesting in many systems. They often correspond to rare events that change the global structure and/or the functional behavior of the system. For example, in macromolecular systems, the slowest events often correspond to functional conformational changes such as folding, binding or catalysis [24, 40, 7, 18]. Therefore, a method is sought that models the slow dynamical processes of continuous-time Markov processes accurately and ideally in a way that supports the efficient simulation of these processes without the need to solve the full direct numerical simulation problem.

Especially in statistical physics, many theories and methods have been proposed to model slow dynamical processes. Examples are rate theories that describe the passage rate of a process across a surface that separates metastable states [13, 17], pathway-based theories and methods that describe the transition dynamics of a system from a subset A to a subset B of state space [12, 3, 21] and network-based approaches that attempt to coarse-grain the high-dimensional dynamics to a network of discrete jump events between sub-states or landmarks [42, 43]. These approaches usually assume a separation of timescales between the slow and the fast processes that results from vanishing smallness parameters (e.g. noise intensity, temperature). In these cases, the mathematical analysis can be based on large deviation estimates and variational principles [14, 12].

In this article, we consider a more general approach to describing slow dynamical processes. Without requiring a separation of timescales, Eq. (1.1) can be decomposed into the propagator's spectral components

$$(1.2) \qquad p_\tau \;=\; \mu + \sum_{i=2}^{m} a_i(p_0)\lambda_i(\tau)l_i + \mathcal{P}_{\text{fast}}(\tau)\, p_0$$

where $\mu, l_2, l_3, ...$ are the propagator's eigenfunctions and $\lambda_i(\tau) = \exp(-\kappa_i \tau)$ (sorted in non-ascending order) are the propagator's eigenvalues that decay exponentially in time with rates κ_i. $a_i(p_0)$ are factors depending on the initial density p_0. We here consider the situation that the eigenspaces of slow and fast processes are orthogonal. For example, in the important case that the system studied is a microscopic physical system in thermal equilibrium, such that the process $\mathbf{z}_t$ is reversible with respect to the invariant density μ, the eigenspaces of slow and fast processes are orthogonal for any choice of m. In such a case, m is a model parameter that can be chosen to distinguish the m slow processes of interest from the fast processes $\mathcal{P}_{\text{fast}}(\tau)$ that are not of interest. For initial densities $p_0 \in \text{span}\{\mu, l_2, ..., l_m\}$, the term for fast processes in Eq. (1.2) vanishes and the propagation can be performed exactly using only the dominant eigenfunctions. Note that Eq. (1.2) represents the formulation of the dynamical process problem as a multi-scale problem in time: μ represents the timescale ∞, $t_2 = \kappa_2^{-1} = -\tau/\ln \lambda_2$ is the slowest dynamical process, etc. This formulation thus allows essential characteristics of the dynamical process to be described by treating its scales *separately*. The relation between dominant eigenvalues, exit times and rates, and metastable sets has been studied by asymptotic expansions in certain smallness parameters as well as by functional analytic means without any relation to smallness parameters [19, 10, 41, 4, 5].

The task is now to approximate the propagator's dominant eigenfunctions $\mu, l_2, l_3, ...$ and eigenvalues λ_i. In other disciplines, variational principles have been worked out in order to approximate eigenfunctions and eigenvalues of known operators such as a quantum-mechanical Hamiltonian [38]. In contrast, for many complex dynamical systems, $\mathcal{P}(\tau)$ is either not known explicitly, or not available in a form that can be transformed into Eq. (1.2). Instead, $\mathcal{P}(\tau)$ is given implicitly through stochastic realizations of the process $\mathbf{z}_t$. Therefore, a variational principle is sought that allows eigenfunctions $\mu, l_2, l_3, ...$ and eigenvalues λ_i to be approximated through statistical observables of $\mathbf{z}_t$. Such a variational principle will be formulated in the present paper.

This problem has extensively been studied for specific functional forms of the eigenfunctions l_i. When l_i are approximated via characteristic functions on a given set decomposition of state space, i.e. $l_i \in \text{span}\{\mathbf{1}_{S_1}, ..., \mathbf{1}_{S_n}\}$ with $S_j \subset \Omega$, the problem of finding the best approximation to eigenfunctions and eigenvalues is solved by a Markov model or Markov state model (MSM) [31, 4, 10, 30, 23]. In another version of MSMs, l_i are approximated by committor functions between a few pre-defined "cores" that form a non-complete subset of state space [8, 11, 32]. Basis functions that form a partition of unity are used in [44]. Markov state models have been recently used a lot to model molecular dynamics processes, especially in conjunction with large amounts of distributedly simulated trajectory [37, 35, 9, 22, 8, 24]. Applications include conformational rearrangements and folding of peptides, proteins and RNA [9, 25, 6, 24, 40, 23]. In this application area, MSMs have had significant impact because they can be estimated from relatively short simulation trajectories and yet allow the system behavior to be predicted at long timescales. Despite this success, significant challenges remain. For example, in most current applications, the discretization of state space is done heuristically *via* a Voronoi partition of state space obtained from clustering available data points. The ability to construct a state space discretization adaptively would tremendously aid the construction of MSMs that are precise while avoiding the use of too many states. Such an adaptive discretization must be guided by an objective function that somehow measures the error made by the model. A bound to the MSM discretization error has been derived in [30]. However, this error is not suitable to design a constructive discretization approach as its evaluation requires knowledge of the exact eigenfunctions. The variational principle derived in this paper only uses statistical observables and is henceforth the basis for such a constructive approach to adaptive discretization.

The article is organized as follows: In Sec. 2 a variational principle is formulated where the dominant eigenfunctions of stochastic dynamical systems are approximated by maximizing a Raleigh coefficient, which - in the limit of the exact solution - is identical to the true eigenvalues. This Raleigh coefficient is linked to the computation of correlation functions that can be evaluated without explicit knowledge of the propagator $\mathcal{P}$. Sec. 3 makes considerations which types functions may be practically useful to construct an approximation to Eq. (1.2) in complex systems. Sec. 4 shows numerical experiments on

a diffusion process in a one-dimensional double-well potential. Sec. 5 concludes this study and makes suggestions for the next steps.

2. Variational principle for conformation dynamics

2.1. Basics.
Let Ω be a real-valued vector space $\mathbb{R}^d$ (state space) and μ, p, l, r functions on a Hilbert space $\mathcal{H} = \{p : \Omega \to \mathbb{R} : \int_\Omega d\mathbf{x}\, p^2(\mathbf{x}) < \infty\}$ with scalar product $\langle u, v \rangle_w = \int_\Omega d\mathbf{x}\, u(\mathbf{x})\, v(\mathbf{x})\, w(\mathbf{x})$. We consider a Markov process $\mathbf{z}_t$ on Ω which is stationary and ergodic with respect to its unique stationary (invariant) distribution $\mu(\mathbf{x}) \equiv p(\mathbf{z}_t = \mathbf{x})\, \forall t$. We use variables $\mathbf{x}, \mathbf{y} \in \Omega$ to denote points in state space. The dynamics of the process $\mathbf{z}_t$ are characterized by the transition density

$$(2.1) \qquad p(\mathbf{x}, \mathbf{y}; \tau) = p(\mathbf{z}_{t+\tau} = \mathbf{y} \mid \mathbf{z}_t = \mathbf{x}),$$

and the correlation density, i.e., the probability density of finding the process at points $\mathbf{x}$ and $\mathbf{y}$ at a time spacing of τ, is defined by

$$(2.2) \qquad C(\mathbf{x}, \mathbf{y}; \tau) = \mu(\mathbf{x})\, p(\mathbf{x}, \mathbf{y}; \tau) = p(\mathbf{z}_{t+\tau} = \mathbf{y},\, \mathbf{z}_t = \mathbf{x}).$$

We further assume $\mathbf{z}_t$ to be reversible with respect to its stationary distribution, i.e.:

$$(2.3) \qquad \mu(\mathbf{x})\, p(\mathbf{x}, \mathbf{y}; \tau) \;=\; \mu(\mathbf{y})\, p(\mathbf{y}, \mathbf{x}; \tau)$$

$$(2.4) \qquad C(\mathbf{x}, \mathbf{y}; \tau) \;=\; C(\mathbf{y}, \mathbf{x}; \tau).$$

Reversibility is not strictly necessary but tremendously simplifies the forthcoming expressions and their interpretation [30]. In physical simulations, reversibility is the consequence of the simulation system being in thermal equilibrium with its environment, i.e. the dynamics in the system is purely a consequence of thermal fluctuations and there are no external driving forces.

Consider a probability density $p_t(\mathbf{x}) \equiv p(\mathbf{z}_t = \mathbf{x})$. We can write the propagation of this density *via* propagator $\mathcal{P}(\tau)$ as:

$$(2.5) \qquad p_\tau(\mathbf{y}) = \mathcal{P}(\tau) \circ p_0(\mathbf{x}) = \int_{\mathbf{x}} d\mathbf{x}\, p_0(\mathbf{x})\, p(\mathbf{x}, \mathbf{y}; \tau)$$

2.2. Spectral decomposition.
The transition density can be decomposed into spectral components of the propagator [30]:

$$(2.6) \qquad p(\mathbf{x}, \mathbf{y}; \tau) = \sum_{i=1}^{m} \lambda_i(\tau)\, \mu^{-1}(\mathbf{x})\, l_i(\mathbf{x})\, l_i(\mathbf{y}) + p_{\text{fast}}(\mathbf{x}, \mathbf{y}; \tau)$$

where l are eigenfunctions and λ_i are eigenvalues of the propagator, i.e.

$$(2.7) \qquad \lambda_i(\tau)\, l_i = \mathcal{P}(\tau)\, l_i.$$

and eigenvalues shall be sorted as $\lambda_1 = 1 > \lambda_2 \geq \lambda_3 \ldots$. The eigenfunctions are normalized by:

$$(2.8) \qquad \langle l_i, l_j \rangle_{\mu^{-1}} = \int_{\mathbf{x}} d\mathbf{x}\, \mu^{-1}(\mathbf{x})\, l_i(\mathbf{x})\, l_j(\mathbf{x}) \;=\; \delta_{ij}.$$

where δ_{ij} is the Kronecker delta. For the first term we have

$$(2.9) \qquad l_1 = \mathcal{P}(\tau)\, l_1,$$

i.e. l_1 is proportional to the stationary (invariant) density. As a result of the normalization conditions we have $\|l_i\|_1 = \int_{\mathbf{x}} d\mathbf{x}\, l_i(\mathbf{x}) = 1$ and

$$(2.10) \qquad l_1(\mathbf{x}) = \mu(\mathbf{x})$$

is identical to the stationary density. As a result of reversibility, the fast part p_{fast} vanishes for long times τ and we are left with:

$$(2.11) \qquad p(\mathbf{x}, \mathbf{y}; \tau) \;=\; \sum_{i=1}^{m} \lambda_i(\tau)\, \mu^{-1}(\mathbf{x})\, l_i(\mathbf{x})\, l_i(\mathbf{y})$$

$$(2.12) \qquad \;=\; \sum_{i=1}^{m} \exp(-\kappa_i \tau)\, \mu^{-1}(\mathbf{x})\, l_i(\mathbf{x})\, l_i(\mathbf{y})$$

where κ_i is an implied rate. Correspondingly, the correlation density can be written as:

$$(2.13) \qquad C(\mathbf{x}, \mathbf{y}; \tau) = \sum_{i=1}^{m} \lambda_i(\tau)\, l_i(\mathbf{x})\, l_i(\mathbf{y})$$

2.3. **Raleigh variational principle.** In nontrivial dynamical systems neither the correlation densities $p(\mathbf{x}, \mathbf{y}; \tau)$ and $C(\mathbf{x}, \mathbf{y}; \tau)$ nor the eigenvalues λ_i and eigenfunctions l_i are analytically available. This section provides a variational principle based on which these quantities can be estimated from simulation data generated by the dynamical process $\mathbf{z}_t$. For this, the formalism introduced above is used to formulate the Raleigh variational principle used in quantum mechanics [38] for Markov processes.

The density $C(\mathbf{x}, \mathbf{y}; \tau)$ is considered to act as a the kernel of a correlation operator. Let f be a real-valued function of state, $f = f(\mathbf{x}) : \Omega \to \mathbb{R}$, its autocorrelation with respect to the stochastic process $\mathbf{z}_t$ is given by:

$$(2.14) \qquad \mathrm{acf}(f; \tau) \quad = \quad \mathbb{E}[f(\mathbf{z}_0)\, f(\mathbf{z}_\tau)] = \int_\mathbf{x} \int_\mathbf{y} d\mathbf{x}\, d\mathbf{y}\, f(\mathbf{x})\, C(\mathbf{x}, \mathbf{y}; \tau)\, f(\mathbf{y})$$

Remark 1. In the Dirac notation often used in physical literature, integrals such as the one above may be abbreviated by $\mathbb{E}[f(\mathbf{x}_0)\, f(\mathbf{x}_\tau)] = \langle f \mid \mathcal{C} \mid f \rangle$ with the correlation operator defined as $\mid \mathcal{C} \mid f \rangle = \int_\mathbf{x} d\mathbf{x}\, f(\mathbf{x})\, C(\mathbf{x}, \mathbf{y}; \tau)$.

Theorem 2. The autocorrelation function of a weighted eigenfunction $r_k = \mu^{-1} l_k$ is its eigenvalue λ_k:

$$(2.15) \qquad \mathrm{acf}(r_k; \tau) = \mathbb{E}\left[r_k(\mathbf{z}_0)\, r_k(\mathbf{z}_\tau)\right] = \lambda_k$$

Proof. Using (2.14) with $f = \mu^{-1} l_k$, it directly follows that:

$$
\begin{aligned}
(2.16) \qquad \mathrm{acf}(r_k; \tau) \quad &= \quad \int_\mathbf{x} \int_\mathbf{y} d\mathbf{x}\, d\mathbf{y}\, \mu^{-1}(\mathbf{x})\, l_k(\mathbf{x})\, C(\mathbf{x}, \mathbf{y}; \tau)\, \mu^{-1}(\mathbf{y})\, l_k(\mathbf{y}) \\
&= \quad \sum_{i=1}^m \lambda_i(\tau) \int_\mathbf{x} \int_\mathbf{y} d\mathbf{x}\, d\mathbf{y}\, \mu^{-1}(\mathbf{x})\, l_k(\mathbf{x})\, l_i(\mathbf{x})\, l_i(\mathbf{y})\, \mu^{-1}(\mathbf{y})\, l_k(\mathbf{y}) \\
&= \quad \sum_{i=1}^m \lambda_i(\tau)\, \langle l_k, l_i \rangle^2_{\mu^{-1}} \\
&= \quad \sum_{i=1}^m \lambda_i(\tau)\, \delta_{ik} \\
&= \quad \lambda_k(\tau).
\end{aligned}
$$

$\square$

Theorem 3. Let $\hat{r}_2 = \mu^{-1} \hat{l}_2$ be an approximate model for the second eigenfunction, which is normalized and orthogonal to the true first eigenfunction:

$$(2.17) \qquad \langle \hat{l}_2, \mu \rangle_{\mu^{-1}} \quad = \quad 0$$
$$(2.18) \qquad \langle \hat{l}_2, \hat{l}_2 \rangle_{\mu^{-1}} \quad = \quad 1,$$

then

$$(2.19) \qquad \mathrm{acf}(\hat{r}_2; \tau) = \mathbb{E}\left[\hat{r}_2(\mathbf{z}_0)\, \hat{r}_2(\mathbf{z}_\tau)\right] \leq \lambda_2$$

Proof. $\hat{l}_2$ is written in terms of the basis of eigenfunctions l_i:

$$(2.20) \qquad \hat{l}_2 = \sum_i a_i l_i.$$

Due to $\langle \hat{l}_2, \mu \rangle_{\mu^{-1}} = \langle \hat{l}_2, 1 \rangle = 0$, $\mu(x) \geq 0$, and $\mu^{-1} \hat{l}_2 = \sum_i a_i \mu^{-1} l_i = a_1 1 + \sum_{i \geq 2} a_i \mu^{-1} l_i$ it follows $a_1 = 0$. Hence:

$$(2.21) \qquad \hat{l}_2 = \sum_{i \geq 2} a_i l_i = a_2 l_2 + \sum_{i > 2} a_i l_i = a_2 l_2 + \epsilon.$$

Using the normalization condition (2.18), the following equality can be derived for the amplitudes:

$$
\begin{aligned}
1 &= \langle \hat{l}_2, \hat{l}_2 \rangle_{\mu^{-1}} \\
&= \langle \sum_{i\geq 2} a_i l_i, \sum_{j\geq 2} a_j l_j \rangle_{\mu^{-1}} \\
&= \sum_{i\geq 2} a_i \sum_{j\geq 2} a_j \langle l_i, l_j \rangle_{\mu^{-1}} \\
&= \sum_{i\geq 2} a_i^2
\end{aligned}
$$

(2.22)

then

$$
\begin{aligned}
\mathrm{acf}(\mu^{-1}\hat{l}_2; \tau) &= \sum_i \lambda_i(\tau) \int_{\mathbf{x}} \int_{\mathbf{y}} d\mathbf{x}\, d\mathbf{y}\, \mu^{-1}(\mathbf{x}) \left(\sum_{j\geq 2} a_j l_j(\mathbf{x}) \right) l_i(\mathbf{x})\, l_i(\mathbf{y})\, \mu^{-1}(\mathbf{y}) \left(\sum_{j\geq 2} a_j l_j(\mathbf{y}) \right) \\
&= \sum_i \lambda_i(\tau) \left[\int_{\mathbf{x}} d\mathbf{x}\, \mu^{-1}(\mathbf{x}) \left(\sum_{j\geq 2} a_j l_j(\mathbf{x}) \right) l_i(\mathbf{x}) \right]^2 \\
&= \sum_i \lambda_i(\tau) \left[\sum_{j\geq 2} a_j \langle l_j, l_i \rangle_{\mu^{-1}} \right]^2 \\
&= \sum_i a_i^2 \lambda_i(\tau) \\
&= a_2^2 \lambda_2(\tau) + \sum_i a_i^2 \lambda_i(\tau) \\
&\leq a_2^2 \lambda_2(\tau) + \sum_i a_i^2 \lambda_2(\tau) = \lambda_2(\tau) \sum_i a_i^2 = \lambda_2(\tau)
\end{aligned}
$$

(2.23)

$\square$

Corollary 4. Let $\hat{r}_k = \mu^{-1}\hat{l}_k$ be an approximate model for the k'th eigenfunction, with the normalization and orthogonality constraints:

$$
\begin{aligned}
\langle \hat{l}_k, l_i \rangle_{\mu^{-1}} &= 0, \quad \forall i < k \\
\langle \hat{l}_k, \hat{l}_k \rangle_{\mu^{-1}} &= 1,
\end{aligned}
$$

(2.24)

then

$$
\mathrm{acf}(\hat{r}_k; \tau) = \mathbb{E}\left[\hat{r}_k(\mathbf{z}_0)\, \hat{r}_k(\mathbf{z}_\tau) \right] \leq \lambda_k
$$

(2.25)

The proof is analogous to Theorem 3, with Eq. (2.22) being $\sum_{i\geq k} a_i^2 = 1$.

Remark 5. A crucial assumption of the variational principle given by Theorems (2) to (4) is that for estimating the k-th eigenfunction, the $k-1$ dominant eigenfunctions are already known. In particular, the first eigenfunction, i.e. the stationary density must be known. In practice, these eigenfunctions are approximated via solving a variational principle. Nonetheless, some basic statements can be made even if no eigenfunction is known exactly. For example, it is trivial that when the estimated stationary density $\hat{\mu}$ is used in Theorem 2, then the estimate of the first eigenvalue is still always correctly 1:

$$
\mathrm{acf}(\hat{\mu}^{-1}\hat{\mu}; \tau) = \mathrm{acf}(1; \tau) = 1
$$

(2.26)

and from theorems 2 and 3 it follows that any function $\hat{r}_k \neq \hat{\mu}$

$$
\mathrm{acf}(\hat{r}_k; \tau) < 1
$$

(2.27)

hence the eigenvalue 1 is simple and dominant also when estimating eigenvalues from data.

Remark 6. An important insight at this point is that a variational principle of conformation dynamics can be formulated in terms of correlation functions. In contrast to quantum mechanics or other fields where the variational principle has been successfully employed, no closed-form expression of the operator $\mathcal{C}$ is needed. The ability to express the variational principle in terms of correlation functions with respect to $\mathcal{C}$, means that the eigenvalues to be maximized can be directly estimated from

simulation data. When statistically sufficiently realizations of $\mathbf{z}_t$ are available, then the autocorrelation function can be estimated via:

$$\text{(2.28)} \qquad \text{acf}(\hat{r}_k; \tau) = \mathbb{E}(\hat{r}_k(\mathbf{z}_0)\hat{r}_k(\mathbf{z}_\tau)) \approx \frac{1}{N} \sum \hat{r}_k(\mathbf{z}_0)\hat{r}_k(\mathbf{z}_\tau)$$

where N are the number of simulated time windows of length τ.

2.4. **Ritz method.** The Ritz method is a systematic approach to find the best possible approximation to the m first eigenfunctions of an operator $\mathcal{C}$ simultaneously in terms of a linear combination of orthonormal functions [28]. Here the Ritz method is simply restated in terms of the present notation. Let $\chi_i : \Omega \to \mathbb{R}$, $i \in \{1, ..., m\}$ be a set of m orthonormal basis functions:

$$\text{(2.29)} \qquad \langle \chi_i, \chi_j \rangle_\mu = \delta_{ij}$$

and let $\boldsymbol{\chi}$ denote the vector of these functions:

$$\text{(2.30)} \qquad \boldsymbol{\chi}(\mathbf{x}) = [\chi_1(\mathbf{x}), ..., \chi_m(\mathbf{x})]^T.$$

We seek a coefficient matrix $\mathbf{B} \in \mathbb{R}^{m \times m}$ with

$$\text{(2.31)} \qquad \mathbf{B} = [\mathbf{b}_1, ..., \mathbf{b}_m]$$

with the column vectors $\mathbf{b}_i = [b_{i1}, ..., b_{im}]^T$ that approximate eigenfunctions of operator $\mathcal{C}$ as:

$$\text{(2.32)} \qquad \hat{r}_i(\mathbf{x}) = \mu^{-1}(\mathbf{x})\hat{l}_i(\mathbf{x}) \quad = \quad \mathbf{b}_i^T \boldsymbol{\chi}(\mathbf{x}) = \langle \mathbf{b}_i, \boldsymbol{\chi}(\mathbf{x}) \rangle$$

The matrix $\mathbf{B}$ that optimally approximates the eigenfunctions in terms of maximizing the Raleigh coefficients $\hat{\lambda}_i(\tau) = \text{acf}(\hat{\mu}^{-1}\hat{l}_i; \tau)$ is found by the eigenvectors of the eigenvalue problem:

$$\text{(2.33)} \qquad \mathbf{HB} = \mathbf{B\Lambda}$$

with the individual eigenvalue/eigenvector pairs

$$\text{(2.34)} \qquad \mathbf{Hb}_i = \mathbf{b}_i \hat{\lambda}_i$$

and the density matrix $\mathbf{H} = [h_{ij}]$ with:

$$\text{(2.35)} \qquad h_{ij} \quad = \quad \int_{\mathbf{x}} \int_{\mathbf{y}} d\mathbf{x} \, d\mathbf{y} \, \chi_i(\mathbf{x}) \, C(\mathbf{x}, \mathbf{y}; \tau) \, \chi_j(\mathbf{y})$$

$$\text{(2.36)} \qquad \quad = \quad \mathbb{E}[\chi_i(\mathbf{z}_0) \, \chi_j(\mathbf{z}_\tau)],$$

or $h_{ij} = \langle \chi_i \, | \, \mathcal{C} \, | \, \chi_j \rangle$ in the Dirac notation.

Remark 7. Due to the equality between Eq. (2.35) and (2.36) the elements of the $\mathbf{H}$ matrix can be estimated as correlation functions of a simulation of the process $\mathbf{z}_t$

2.5. **Markov state model.** Let $\{S_1, ..., S_n\}$ be pairwise disjoint sets partitioning Ω and let $\pi_i = \int_{S_i} d\mathbf{x}\mu(\mathbf{x})$ be the stationary probability of set $S_i \subset \Omega$. Consider the piecewise constant functions

$$\text{(2.37)} \qquad \chi_i = \frac{1}{\sqrt{\pi_i}} \mathbf{1}_{S_i}$$

where $\mathbf{1}_{S_i}$ is the characteristic function that is 1 for $\mathbf{x} \in S_i$ and 0 elsewhere. Since $S_i \cap S_j = \emptyset$ for all $i \neq j$ these functions form a basis set with $\langle \chi_i, \chi_j \rangle_\mu = \delta_{ij}$. The corresponding $\mathbf{H}$ matrix evaluates to

$$\text{(2.38)} \qquad \begin{aligned} h_{ij} \quad &= \quad \frac{1}{\sqrt{\pi_i \pi_j}} \int_{\mathbf{x}} \int_{\mathbf{y}} d\mathbf{x} \, d\mathbf{y} \, \mathbf{1}_{S_i} C(\mathbf{x}, \mathbf{y}; \tau) \, \mathbf{1}_{S_i} \\ &= \quad \frac{1}{\sqrt{\pi_i \pi_j}} \int_{S_i} \int_{S_j} d\mathbf{x} \, d\mathbf{y} \, C(\mathbf{x}, \mathbf{y}; \tau) \\ &= \quad \frac{c_{ij}}{\sqrt{\pi_i \pi_j}} \\ &= \quad T_{ij} \sqrt{\frac{\pi_i}{\pi_j}} \end{aligned}$$

where $c_{ij} = \mathbb{P}(\mathbf{z}_{t+\tau} \in S_j, \mathbf{z}_t \in S_i)$ is the joint probability of observing the process in sets S_i and S_j with a time lag of τ while $T_{ij} = \mathbb{P}(\mathbf{z}_{t+\tau} \in S_j \mid \mathbf{z}_t \in S_i)$ is the corresponding transition probability. The optimal approximation to eigenfunctions $\hat{\mu}^{\frac{1}{2}}\hat{l}_i = \langle \mathbf{b}_i, \boldsymbol{\chi} \rangle$ is given by the Ritz method as

$$\text{(2.39)} \qquad \mathbf{\Pi}^{\frac{1}{2}} \mathbf{T} \mathbf{\Pi}^{-\frac{1}{2}} \mathbf{B} = \mathbf{B\Lambda}$$

where $\mathbf{\Pi} = \mathrm{diag}(\pi_1, ..., \pi_n)$, and, equivalently

$$\text{(2.40)} \qquad\qquad\qquad \mathbf{TR} = \mathbf{R\Lambda}$$

with $\mathbf{R} = \mathbf{\Pi}^{-\frac{1}{2}}\mathbf{B} = (\mathbf{r}_1, ..., \mathbf{r}_n)$ are the coefficients forming the step-functions $\hat{r}_i = \hat{\mu}^{-1}\hat{l}_i = \langle \mathbf{r}_i, \boldsymbol{\chi} \rangle$ that approximate $r_i = \mu^{-1}l_i$. Thus, the eigenvectors and eigenvalues of the Markov model transition matrix $\mathbf{T} = [T_{ij}]$ are the optimal step-function approximation to the true eigenfunctions $r_i = \mu^{-1}l_i$ and eigenvalues λ_i. This conclusion can also be obtained from Ref. [30] *via* a different route.

2.6. Roothaan-Hall method.
The Roothaan-Hall method is a generalization of the Ritz method used for solving the linear parameter optimization problem for the case when the basis set is not orthogonal [29, 16]. Let the matrix $\mathbf{S} \in \mathbb{R}^{m \times m}$ with elements

$$\text{(2.41)} \qquad\qquad\qquad S_{ij} = \langle \chi_i, \chi_j \rangle$$

be the matrix of overlap integrals with the normalization conditions $S_{ii} = 1$. Note that $\mathbf{S}$ has full rank if and only if all χ_i are pairwise linearly independent. The optimal solution $\mathbf{B}$ in the sense of Eqs (2.31)-(2.32) is found by the eigenvectors of the generalized eigenvalue problem:

$$\text{(2.42)} \qquad\qquad\qquad \mathbf{HB} = \mathbf{SB\Lambda}$$

with the individual eigenvalue/eigenvector pairs:

$$\text{(2.43)} \qquad\qquad\qquad \mathbf{Hb}_i = \mathbf{Sb}_i\hat{\lambda}_i$$

The direct approach to solve this problem is given by

$$\text{(2.44)} \qquad\qquad\qquad \mathbf{S}^{-1}\mathbf{HC} = \mathbf{C\Lambda}.$$

Remark 8. The Ritz and Roothaan-Hall methods are useful for eigenfunction models that are expressed in terms linear combinations of basis functions. Non-linear parameter models can also be handled with nonlinear optimization methods. In such nonlinear cases it needs to be tested whether there is a unique optimum or not.

3. Modeling

Section 2 has provided a general variational principle for approximating the dominant eigenvalues and eigenfunctions of Markov processes. In order to apply this principle to complex systems, a useful level of modeling the eigenfunctions in terms of basis functions needs to be found, and appropriate classes of basis functions must be identified. This sections attempt a first approach to this problem by making general considerations for what modeling schemes might be appropriate.

3.1. Half-weighted eigenfunctions.
Is it beneficial to directly model the propagator eigenfunctions l_k, their weighted counterparts $r_k = \mu^{-1}l_k$ or rather yet another set of functions? We would like to use a model that has the following properties:

(1) As basis functions χ_i it is preferred to use local functions, i.e. either functions with compact support, or at least with the property $\lim_{|\mathbf{x}| \to \infty} \chi_i(\mathbf{x}) \to 0$. Such locality is useful to direct the computation effort to specific regions of state space and may aid the adaptive refinement of the eigenfunction approximation by specifically adding basis functions that add local refinements. Since we also aim at modeling eigenfunctions as linear combinations of basis functions we cannot use the r_k eigenfunctions that are not local.

(2) We would like to be able to pre-compute as many expressions as possible analytically. When using appropriate basis functions χ_i and χ_j it may be possible to calculate analytic solutions of the integrals $\langle \chi_i, \chi_j \rangle$, albeit this feature is usually destroyed when weighting with the stationary density as in $\langle \chi_i, \chi_j \rangle_{\mu^{-1}}$. Therefore we will also avoid using the eigenfunctions l_k that would require such a weighting.

Consider a rewrite of Eq. (2.16) as:

$$\mathrm{acf}(r_k; \tau) = \int_{\mathbf{x}} \int_{\mathbf{y}} d\mathbf{x}\, d\mathbf{y}\, \mu^{-\frac{1}{2}}(\mathbf{x})\, l_k(\mathbf{x})\, \mu^{-\frac{1}{2}}(\mathbf{x})\, C(\mathbf{x}, \mathbf{y}; \tau)\, \mu^{-\frac{1}{2}}(\mathbf{y})\, \mu^{-\frac{1}{2}}(\mathbf{y})\, l_k(\mathbf{y})$$

$$\text{(3.1)} \qquad\qquad = \int_{\mathbf{x}} \int_{\mathbf{y}} d\mathbf{x}\, d\mathbf{y}\, \phi_k(\mathbf{x})\, S(\mathbf{x}, \mathbf{y}; \tau)\, \phi_k(\mathbf{y})$$

where the "half-weighted" eigenfunctions:

$$(3.2) \qquad \phi_i(\mathbf{x}) = \frac{l_i(\mathbf{x})}{\mu^{\frac{1}{2}}(\mathbf{x})},$$

and the "half-weighted" correlation density:

$$(3.3) \qquad S(\mathbf{x}, \mathbf{y}; \tau) = \frac{C(\mathbf{x}, \mathbf{y}; \tau)}{\mu^{\frac{1}{2}}(\mathbf{x})\mu^{\frac{1}{2}}(\mathbf{y})}$$

have been defined. When now modeling the half-weighted eigenfunctions ϕ_i using some basis set, the following nice properties are obtained:

(1) Local basis functions can be used. This follows from $\lim_{|\mathbf{x}|\to\infty} \phi_i(\mathbf{x}) = \lim_{|\mathbf{x}|\to\infty} \mu^{\frac{1}{2}}(\mathbf{x})r_i(\mathbf{x}) \to 0$

(2) The normalization condition requires a non-weighted scalar product:

$$
\begin{aligned}
(3.4) \qquad \langle l_i, l_j \rangle_{\mu^{-1}} &= \left\langle \frac{l_i}{\mu^{1/2}}, \frac{l_j}{\mu^{1/2}} \right\rangle \\
&= \langle \phi_i, \phi_j \rangle = \delta_{ij}.
\end{aligned}
$$

(3) When $\langle \chi_i, \chi_j \rangle$ is analytically computable and $\phi_k = \sum_i c_i \chi_i$, then $\langle \phi_k, \phi_k \rangle$ is also analytically computable.

(4) The first half-weighted eigenfunction has eigenvalue 1 and is identical to the half-weighted stationary density

$$(3.5) \qquad \phi_1(\mathbf{x}) = \frac{l_1(\mathbf{x})}{\mu(\mathbf{x})^{1/2}} = \mu(\mathbf{x})^{1/2}.$$

(5) When models of $\mu(\mathbf{x})^{1/2}$ and ϕ_k are available, the Raleigh coefficient in Eq. (3.1) can be estimated numerically as the autocorrelation of $\frac{\phi_i}{\mu^{1/2}}$

(6) When defining a propagator $\mathcal{P}^*$ in half-weighted space via:

$$
\begin{aligned}
(3.6) \qquad p_\tau(\mathbf{y}) &= \mathcal{P}(\tau) \circ p_0(\mathbf{x}) \\
p_\tau(\mathbf{y}) &= \int_{\mathbf{x}} d\mathbf{x}\, p(\mathbf{x})\, p(\mathbf{x}, \mathbf{y}; \tau) \\
\frac{p_\tau(\mathbf{y})}{\mu(\mathbf{y})^{1/2}} &= \int_{\mathbf{x}} d\mathbf{x}\, \frac{p(\mathbf{x})}{\mu(\mathbf{x})^{1/2}} \frac{\mu(\mathbf{x})^{1/2}}{\mu(\mathbf{y})^{1/2}}\, p(\mathbf{x}, \mathbf{y}; \tau) \\
p_\tau^*(\mathbf{y}) &= \int_{\mathbf{x}} d\mathbf{x}\, p_0^*(\mathbf{x})\, p^*(\mathbf{x}, \mathbf{y}; \tau) \\
&= \mathcal{P}^*(\tau) \circ p_0^*(\mathbf{x})
\end{aligned}
$$

then $\mathcal{P}^*$ is self-adjoint and has orthogonal eigenfunctions

$$(3.7) \qquad \phi_i \lambda_i = \mathcal{P}^*(\tau) \phi_i$$

It follows from theorem (2) that the exact eigenvalues are calculated by the Raleigh coefficients of the exact eigenfunctions:

$$(3.8) \qquad \lambda_i = \left\langle \mu^{-\frac{1}{2}} \phi_i \mid \mathcal{C} \mid \mu^{-\frac{1}{2}} \phi_i \right\rangle = \mathrm{acf}(\mu^{-\frac{1}{2}} \phi_i; \tau)$$

while they are approximated from below by the Raleigh coefficients of the approximate eigenfunctions:

$$(3.9) \qquad \lambda_i \geq \hat{\lambda}_i = \left\langle \mu^{-\frac{1}{2}} \hat{\phi}_i \mid \mathcal{C} \mid \mu^{-\frac{1}{2}} \hat{\phi}_i \right\rangle = \mathrm{acf}(\mu^{-\frac{1}{2}} \hat{\phi}_i; \tau).$$

This Raleigh-coefficient can be directly sampled: for a given trajectory $\mathbf{z}_t$, it can be estimated as:

$$(3.10) \qquad \lambda_i \geq \hat{\lambda}_i = \mathbb{E}_t \left[\hat{\mu}(\mathbf{z}_t)^{-\frac{1}{2}} \hat{\phi}_i(\mathbf{z}_t) \hat{\mu}(\mathbf{z}_{t+\tau})^{-\frac{1}{2}} \hat{\phi}_i(\mathbf{z}_{t+\tau}) \right]$$

Thus, for a given trajectory $\mathbf{z}_t$, the optimal eigenfunctions $\hat{\phi}_i$ can be calculated by maximizing the Raleigh coefficient, using e.g. the Ritz or the Roothaan-Hall method.

3.2. Gaussian Basis functions.

Let us assume that the state space Ω is a metric space with distance $d(\mathbf{x}, \mathbf{y})$, and let us further consider that the half-weighted invariant density $\mu(\mathbf{x})^{1/2}$ be given in terms of Gaussian basis functions:

$$(3.11) \qquad \mu(\mathbf{x})^{1/2} = \sum_i a_i \exp\left(-\frac{d(\mathbf{x}, \mathbf{y}_i)}{2\sigma^2}\right)$$

where $a_i \in \mathbb{R}$, $\mathbf{y}_i \in \Omega$ and $\sigma \in \mathbb{R}$ are amplitude, mean and shape parameters. The invariant density can then be analytically given:

$$(3.12)\ \mu(x) = \left(\mu(x)^{1/2}\right)^2 = \left(\sum_i a_i \exp\left(-\frac{d(\mathbf{x}, \mathbf{y}_i)}{2\sigma^2}\right)\right)^2$$
$$= \sum_i a_i^2 \exp\left(-\frac{d(\mathbf{x}, \mathbf{y}_i)}{\sigma^2}\right) + \sum_{i<j} 2a_i a_j \exp\left(-\frac{d(\mathbf{x}, \mathbf{y}_i) + d(\mathbf{x}, \mathbf{y}_j)}{2\sigma^2}\right),$$

Furthermore, consider that the half-weighted eigenfunctions be given in terms of the same Gaussian basis:

$$(3.13) \qquad \phi_k(\mathbf{x}) = \sum_i b_{ki} \exp\left(-\frac{d(\mathbf{x}, \mathbf{y}_i)}{2\sigma^2}\right)$$

where b_{ki} must be appropriately chosen to guarantee orthogonality with respect to the invariant density. The corresponding unweighted eigenfunctions r_k are

$$(3.14) \qquad r_k(x) = \frac{\phi_k(x)}{\phi_1(x)} = \frac{\sum_i b_{ki} \exp\left(-\frac{d(\mathbf{x}, \mathbf{y}_i)}{2\sigma^2}\right)}{\sum_i a_i \exp\left(-\frac{d(\mathbf{x}, \mathbf{y}_i)}{2\sigma^2}\right)},$$

which does not have a simple form, but can be evaluated point-wise. In order to enforce the normalization $\langle \phi_k, \phi_l \rangle = \delta_{kl}$ we consider

$$(3.15) \qquad \langle \phi_k, \phi_l \rangle = \int d\mathbf{x} \sum_i \sum_j b_{ki} b_{lj} \exp\left(-\frac{d(\mathbf{x}, \mathbf{y}_i) + d(\mathbf{x}, \mathbf{y}_j)}{2\sigma^2}\right),$$

which can be analytically evaluated when Ω is an Euclidean space.

4. Numerical example

In order to illustrate the variational principle we show a numerical example of a diffusion in a one-dimensional potential. The example is chosen such that it is tractable by direct grid discretization so as to be able to generate a reference solution. Different optimization methods for the variational problem and choices of basis sets are considered and illustrated.

Let $\Omega = \mathbb{R}$ be our state space with points $x \in \Omega$. First, a "Gaussian hat" function is defined *via*:

$$(4.1) \qquad gh(x; a, s) := \exp\left(-\frac{(x-a)^2}{2s^2}\right)$$

where $a \in \mathbb{R}$ is the mean and $s \in \mathbb{R}$ the standard deviation. We define a stationary density from two Gaussians:

$$\mu(x) \quad := \quad \frac{1}{2\sqrt{\pi}} \left(gh(x, -2, 1) + gh(x, 2, 1)\right)$$

The corresponding dimensionless generating potential is given by

$$(4.2) \qquad U(x) = -\ln(\mu(x))$$

which exerts a force on a particle at position x of:

$$(4.3) \qquad f(x) = -\nabla U(x) = \frac{1}{\mu(x)} \frac{d}{dx} \mu(x).$$

Using Smoluchowski dynamics and Euler discretization, a time-step $x \xrightarrow{\tau} y$ is given by

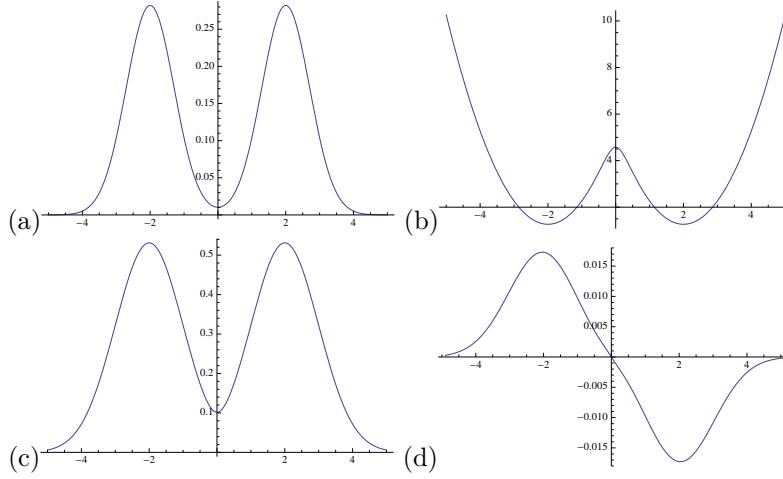$$(4.4) \qquad y = x + \tau f(x) + \sqrt{2\tau}\eta$$

FIGURE 4.1. Two-well potential with Smoluchowski dynamics, $\tau = 0.025$. (a) Double-Gaussian density $\mu(x)$, (b) the corresponding potential $U(x)$, (c) the half-weighted density $\phi_1(x) = \sqrt{\mu(x)}$, (d) slowest-process eigenfunction $\phi_2(x)$ from direct numerical solution.

where η is a Normally distribution random variable (white noise). The transition density can hence be written as:

$$p(x, y; \tau) = \mathcal{N}_y(x + \tau f(x), \sqrt{2\tau}) \tag{4.5}$$

and the correlation density is given by:

$$C(x, y; \tau) = \mu(x)\, p(x, y; \tau) \tag{4.6}$$

Now we are concerned about estimation of eigenfunctions. The first half-weighted eigenfunction is the square root of the stationary density:

$$\phi_1 = \sqrt{\mu(x)} \tag{4.7}$$

such that $\phi_1^2(x) = \mu(x)$. We here assume $\mu(x)$ to be known, although in practice it must be estimated.

4.1. **Ritz method with characteristic functions (Markov state model).** We aim at approximating the eigenvalues and eigenfunctions of the true propagator via the Ritz method described in Sec. 2.4. Here, a basis set $\boldsymbol{\chi} = (\chi_1(x), ..., \chi_N(x))^T$ consisting of $N = 20$ characteristic functions in the range $x \in [-6, 6]$ defined by:

$$\chi_i = \frac{1}{\sqrt{0.6}} \mathbf{1}_{[-6+0.6i,\ -5.4+0.6i]} \tag{4.8}$$

where $\mathbf{1}_{[a,b]}$ is the characteristic function that is 1 on the interval $[a, b]$ and 0 outside. These basis functions are already chosen such that $\langle \chi_i, \chi_j \rangle = \delta_{ij}$. Using the Ritz method with characteristic functions on Markov processes is identical to using a Markov state model. We attempt to approximate eigenfunctions $\hat{\phi}_1 \approx \phi_1$ and $\hat{\phi}_2 \approx \phi_2$ in terms of the linear combination of basis functions:

$$\hat{\phi}_i = \langle \mathbf{b}_i, \boldsymbol{\chi} \rangle. \tag{4.9}$$

This is optimally achieved by seeking the component vectors $\mathbf{b} = (b_1, ..., b_N)^T$ that maximize the Raleigh coefficients

$$\hat{\lambda}_i = \langle \hat{\phi}_i \mid \mathcal{C} \mid \hat{\phi}_i \rangle. \tag{4.10}$$

These components are found by the Eigenvectors of the Eigenvalue problem $\mathbf{H}\mathbf{b}_i = \hat{\lambda}_i \mathbf{b}_i$ with $\mathbf{H} = [h_{ab}] \in \mathbb{R}^{N \times N}$ defined by (Dirac notation):

$$h_{ab} = \langle \chi_a \mid \mathcal{C} \mid \chi_b \rangle. \tag{4.11}$$

For the present characteristic basis functions, h_{ab} takes the form

$$h_{ab} = \frac{\int_{S_a} dx \int_{S_b} dy\, C(x, y; \tau)}{\int_{S_a} dx\, \mu(x)} \tag{4.12}$$

where S_a and S_b are the sets where the characteristic functions χ_a and χ_b are 1.
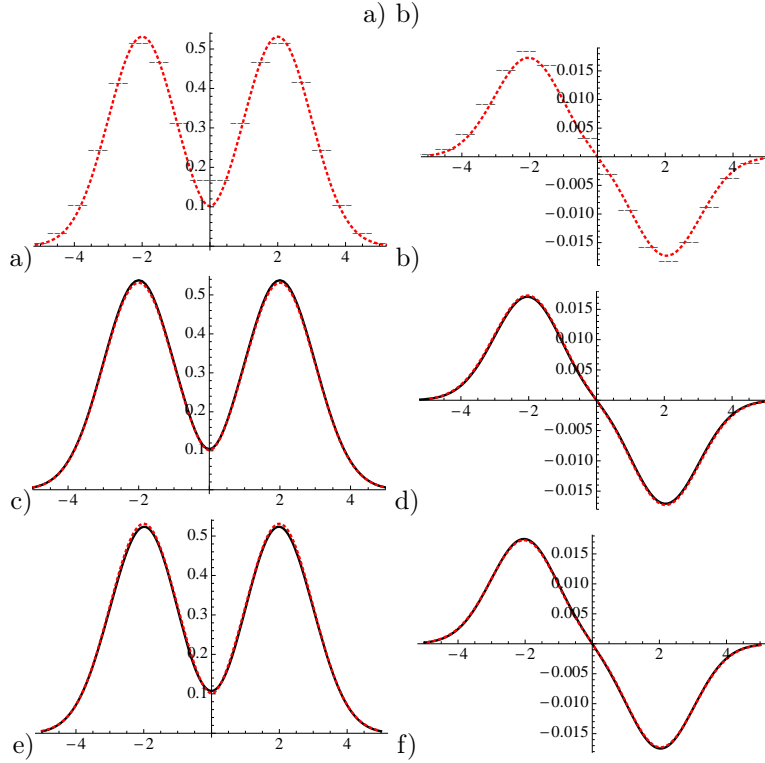
FIGURE 4.2. Approximation to the eigenfunction shown in Fig. 4.1 using different methods and basis sets. The true eigenvalues are 1.0, 0.998913. The reference solutions are shown in red dotted lines while the approximations are shown in black solid lines. a,b) MSM / Ritz method with 20 characteristic functions in the range $x \in [-6, 6]$. Eigenvalues 1.0, 0.980384. c,d) Ritz method with a basis set of 20 Hermite functions, Eigenvalues 1.0, 0.998913. e,f) Roothaan-Hall method with a basis set of 11 Gaussians Eigenvalues 1.0, 0.995507.

The $\mathbf{H}$ matrix was calculated by direct numerical integration using Mathematica and the Eigenvalue problem was subsequently solved, yielding the optimal coefficient vectors $\mathbf{c}_1$ and $\mathbf{c}_2$ that provide the approximations $\hat{\phi}_1 \approx \phi_1$, $\hat{\phi}_2 \approx \phi_2$ and $\hat{\lambda}_1 \approx \lambda_2$, $\hat{\lambda}_2 \approx \lambda_2$. The results are given in Fig. 4.2 a and b, indicating that the eigenvalues are approximated to two significant digits while the eigenfunctions retain a significant discretization error that arises from the step-function basis used.

4.2. **Ritz method with a Hermite basis.** In order to arrive at a smooth solution we employ the Ritz method with a smooth orthogonal function basis. Here, we choose the Hermite functions, defined by:

$$(4.13) \qquad \psi_i(x) = (-1)^i (2^i i! \sqrt{\pi})^{-1/2} e^{x^2/2} \frac{d^i}{dx^i} e^{-x^2}.$$

The Hermite functions are local ($\lim_{|\mathbf{x}| \to \infty} \chi_i(\mathbf{x}) \to 0$) and are thus useful to model the behavior of the eigenfunctions ϕ_k where the stationary density is significantly larger than zero. The basis functions are defined to be the normalized Hermite functions with

$$(4.14) \qquad \chi_i = \frac{\psi_i}{\sqrt{\langle \psi_i, \psi_i \rangle}}.$$

such that $\langle \chi_i, \chi_j \rangle = \delta_{ij}$.

Using the basis set $\boldsymbol{\chi} = [\chi_0, ..., \chi_{19}]^T$, the $\mathbf{H}$ matrix was calculated by direct numerical integration using Mathematica and the Ritz method was used to approximate eigenvalues and eigenfunctions of the propagator. As shown in Fig. 4.2c and d, a nearly perfect approximation of both eigenvalues and eigenfunctions is obtained even though the number of basis functions used is identical to the MSM approach of the previous section. However, the MSM approach has the advantage that it can be employed in high-dimensional spaces which is not the case with Hermite basis functions.

4.3. **Roothaan-Hall method with a Gaussian basis.** In order to have a hope to solve high-dimensional problems, one must resort to simple basis functions, ideally ones with analytical properties that can be practically evaluated in high-dimensional spaces. Therefore, we here suggest the use of Gaussian basis functions as described in Sec. 3.2. In the one-dimensional case, the Gaussians used are:

$$(4.15) \qquad gh_i(x) = \exp\left(-\frac{(x-y_i)^2}{2\sigma^2}\right).$$

Here, we use $\sigma = 1$ and $y_i = (-5, -4, ..., 4, 5)$. Gaussian basis functions are not orthogonal. We therefore calculate the overlap matrix $\mathbf{S} = [s_{ij}]$ with

$$(4.16) \qquad \begin{aligned} s_{ij} &= \langle gh_i, gh_j \rangle \\ &= \int_{-\infty}^{\infty} dx \, \exp\left(-\frac{(x-y_i)^2 + (x-y_j)^2}{2\sigma^2}\right) \end{aligned}$$

that can be evaluated analytically. The $\mathbf{H} = [h_{ab}]$ matrix is again defined by (Dirac notation):

$$(4.17) \qquad h_{ab} = \langle gh_a \mid \mathcal{C} \mid gh_b \rangle.$$

Using the Roothaan-Hall method (Sec. 2.6), the best approximation to the propagator eigenfunctions $\hat{\phi}_i = \langle \mathbf{b}_i, \boldsymbol{\chi} \rangle$ are found by the Eigenvectors of the generalized Eigenvalue problem

$$(4.18) \qquad \mathbf{S}^{-1}\mathbf{H}\mathbf{b}_i = \hat{\lambda}_i \mathbf{b}_i.$$

As shown in Fig. 4.2 c and d, an also nearly perfect approximation of both eigenvalues and eigenfunctions is achieved even though the basis is smaller than the previous basis sets. Since the Gaussian basis set is a good candidate for being used in high-dimensional spaces, this is probably the most useful result so far. Note that the matrix inversion $\mathbf{S}^{-1}$ can be efficiently calculated with sparse matrix methods when a cutoff is used to set nearly-non-overlapping pairs with $h_{ab} \approx 0$ to 0.

4.4. **Nonlinear optimization.** The previous methods used exclusively linear combinations of basis functions. A greater degree of freedom in approximating the propagator eigenfunctions is achieved by using additional shape parameters in the basis functions. This, however, leads to a nonlinear optimization problem that is in general difficult to solve and may have multiple optima. However, we briefly illustrate the approach on our one-dimensional example. We make the Ansatz for the second half-weighted eigenfunction:

$$(4.19) \qquad \begin{aligned} \hat{\phi}_2(x) &= \frac{1}{Z}\left(-gh(x, y_2, s_2) + gh(x, y_2, s_2)\right) \\ Z &= \left[\int_{-\infty}^{\infty} dx \left[-gh(x, y_2, s_2) + gh(x, y_2, s_2)\right]\right]^{1/2} \end{aligned}$$

The normalization constant makes sure that $\langle \phi_2, \phi_2 \rangle = 1$. The constraint $\langle \phi_2, \phi_1 \rangle = 0$ is here ensured by the fact that $\hat{\phi}_1$ is an even function and $\hat{\phi}_2$ is an odd function.

The optimal parameters $\hat{y}_2$ and $\hat{s}_2$ are found by maximizing the Raleigh coefficient:

$$(4.20) \qquad (\hat{y}_2, \hat{s}_2) = \arg\max_{y_2, s_2} \left\langle \frac{\phi_2(y_2, s_2)}{\mu^{1/2}} \mid \mathcal{C} \mid \frac{\phi_2(y_2, s_2)}{\mu^{1/2}} \right\rangle.$$

Fig. 4.3 shows the results of varying y_2 and s_2 as well as the local optimum for $y_2 = 1$ and $s_2 = 0.8$. In this case, a good approximation to the eigenvector could be achieved with a 2-term Ansatz function. However, the general usefulness of the nonlinear approach for high-dimensional problems remains to be evaluated.

5. Conclusions and outlook

Here, we have formulate a variational principle for Markov processes where the dominant eigenfunctions are approximated by maximizing a Raleigh coefficient, which - in the limit of the exact eigenfunctions - is identical to the true eigenvalues. This is the formulation needed to attack the problem of estimating the slow processes in stochastic dynamical systems with a much wider methodology than by the presently used class of Markov State Models. In particular, the entire toolbox of quantum mechanics where many decades of research have gone into the development of eigenfunction approximation methods for high-dimensional systems becomes available.

From a practical point of view, a main achievement of the present study is that the Raleigh coefficient can be estimated from simulation data as it is equivalent to an autocorrelation function of the
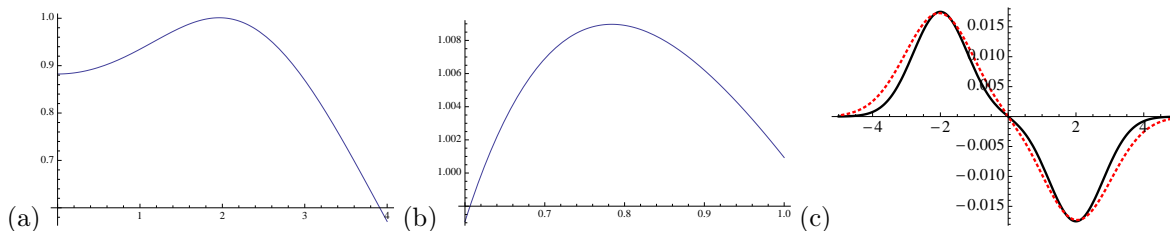
FIGURE 4.3. Nonlinear optimization of the propagator eigenfunctions. (a) value of $\hat{\lambda}_2$ depending on y_2 and with fixed $s_2 = 0.8$. (b) value of $\hat{\lambda}_2$ depending on s_2 with fixed $y_2 = 1$, (c) Approximation to ϕ_2 with $y_2 = 1$, $s_2 = 0.8$ (black), Reference solution for ϕ_2 (red).

appropriately weighted test function. The autocorrelation estimates are such that they can be fed by many short simulations distributed across state space and do not require the direct simulation of the slow processes in a single long trajectory. This is an important advantage in dealing with the sampling problem that arises in simulating metastable dynamical systems.

A main use of the present approach will be to facilitate the development of adaptive discretization algorithms of high-dimensional state spaces for the computational characterization of complex dynamical processes. The Raleigh coefficient derived here represents a practically accessible and theoretically solid functional to guide such an adaptive discretization algorithm. In contrast to Markov state models, such an approximation approach does not necessarily need to use the same basis set for all eigenfunctions. Especially for reversible dynamics, different eigenfunctions can be approximated separately, thus possibly permitting the use of relatively small basis sets.

For a given class of dynamical systems, a basis sets must be selected that is appropriate to model the regularity of the solution. For high-dimensional processes such as molecular dynamics, Gaussian Basis functions might be a workable solution since they be well combined with clustering-based identification of center positions and permit the analytical calculation of some quantities such as the overlap integral. An interesting alternative approach is to build the Basis set upon weakly coupled subsets of internal molecular coordinates, as suggested in the mean field approach developed in Ref. [15]. The usefulness of these and other approaches for complex molecular systems will be investigated in future studies. Furthermore, subsequent studies will deal with statistical considerations, such as the efficient evaluation of uncertainties of the estimated Raleigh coefficients.

REFERENCES

[1] K. Anguige and C. Schmeiser. A one-dimensional model of cell diffusion and aggregation, incorporating volume filling and cell-to-cell adhesion. *Journal of mathematical biology*, 58(3):395–427, March 2009.

[2] Robert B. Best and Gerhard Hummer. Coordinate-dependent diffusion in protein folding. *Proc. Natl. Acad. Sci. USA*, 107(3):1088–1093, January 2010.

[3] Peter G. Bolhuis, David Chandler, Christoph Dellago, and Phillip L. Geissler. Transition path sampling: throwing ropes over rough mountain passes, in the dark. *Annu. Rev. Phys. Chem.*, 53(1):291–318, 2002.

[4] A. Bovier, M. Eckhoff, V. Gayrard, and M. Klein. Metastability in reversible diffusion processes. i. sharp asymptotics for capacities and exit times. *J. Eur. Math. Soc.*, 6:399424, 2004.

[5] A. Bovier, M. Eckhoff, V. Gayrard, and M. Klein. Metastability in reversible diffusion processes. i. precise asymptotics for small eigenvalues. *J. Eur. Math. Soc.*, 7:6999, 2005.

[6] Gregory R. Bowman, Kyle A. Beauchamp, George Boxer, and Vijay S. Pande. Progress and challenges in the automated construction of Markov state models for full protein systems. *J. Chem. Phys.*, 131(12):124101+, September 2009.

[7] Gregory R. Bowman, Vincent A. Voelz, and Vijay S. Pande. Atomistic Folding Simulations of the Five-Helix Bundle Protein Lambda 6-85. *Journal of the American Chemical Society*, 133(4):664–667, February 2011.

[8] Nicaolae V. Buchete and Gerhard Hummer. Coarse Master Equations for Peptide Folding Dynamics. *J. Phys. Chem. B*, 112:6057–6069, 2008.

[9] J. D. Chodera, K. A. Dill, N. Singhal, V. S. Pande, W. C. Swope, and J. W. Pitera. Automatic discovery of metastable states for the construction of Markov models of macromolecular conformational dynamics. *J. Chem. Phys.*, 126:155101, 2007.

[10] P. Deulfhard, W. Huisinga, A. Fischer, and C. Schütte. Identification of almost invariant aggregates in reversibly nearly uncoupled Markov chains. *Lin. Alg. Appl.*, 315:39–59, 2000.

[11] Natasa Djurdjevac, Marco Sarich, and Christof Schütte. Estimating the eigenvalue error of Markov State Models. *Multiscale Model. Simul. (submitted)*, 2010.

[12] Weinan E and E. Vanden Eijnden. *Metastability, conformation dynamics, and transition pathways in complex systems.*, pages 38–65. Multiscale Modelling and Simulation. Springer, 2004.

[13] H. Eyring. The activated complex in chemical reactions. *J. Chem. Phys.*, 3:107–115, 1935.

[14] M. Freidlin and A. D. Wentzell. *Random perturbations of dynamical systems*. Springer, New York, 1998.

[15] G. Friesecke, O. Junge, and P. Koltai. Mean field approximation in conformation dynamics. *Multiscale Model. Simul.*, 8:254–268, 2009.

[16] G. G. Hall. The molecular orbital theory of chemical valency. viii. a method of calculating ionization potentials. *Proceedings of the Royal Society London A*, 205:541–552, 1951.

[17] P. Hänggi, P. Talkner, and M. Borkovec. Reaction Rate Theory: Fifty Years After Kramers. *Rev. Mod. Phys.*, 62:251–342, 1990.

[18] Martin Held, Philipp Metzner, and Frank Noé. Mechanisms of protein-ligand association and its modulation by protein mutations. *Biophys. J.*, 100:701–710, 2011.

[19] R.S. Maier and D.L. Stein. Limiting exit location distribution in the stochastic exit problem. *SIAM J. Appl. Math.*, 57, 1997.

[20] Don L. McLeish and Adam W. Kolkiewicz. *Fitting Diffusion Models in Finance*, volume 32. Institute of Mathematical Statistics, 1997.

[21] P. Metzner, C. Schütte, and E. Vanden-Eijnden. Illustration of transition path theory on a collection of simple examples. *The Journal of chemical physics*, 125(8), August 2006.

[22] F. Noé, I. Horenko, C. Schütte, and J. C. Smith. Hierarchical Analysis of Conformational Dynamics in Biomolecules: Transition Networks of Metastable States. *J. Chem. Phys.*, 126:155102, 2007.

[23] Frank Noé, Sören Doose, Isabella Daidone, Marc Löllmann, John D. Chodera, Markus Sauer, and Jeremy C. Smith. Dynamical fingerprints: Understanding biomolecular processes in microscopic detail by combination of spectroscopy, simulation and theory. *Proc. Natl. Acad. Sci. USA*, 108:4822–4827, 2011.

[24] Frank Noé, Christof Schütte, Eric Vanden-Eijnden, Lothar Reich, and Thomas R. Weikl. Constructing the full ensemble of folding pathways from short off-equilibrium simulations. *Proc. Natl. Acad. Sci. USA*, 106:19011–19016, 2009.

[25] Albert C. Pan and Benoît Roux. Building Markov state models along pathways to determine free energies and rates of transitions. *J. Chem. Phys.*, 129(6):064107+, August 2008.

[26] Jon D. Pelletier. A Stochastic Diffusion Model of Climate Change. *arXiv:ao-sci/9510001*, October 1995.

[27] M. Rieger, J. Rogal M., and K. Reuter. Effect of surface nanostructure on temperature programmed reaction spectroscopy: First-principles kinetic monte carlo simulations of co oxidation at ruo2(110). *Phys. Rev. Lett.*, 100:016105, 2008.

[28] Walter Ritz. Über eine neue methode zur lösung gewisser variationsprobleme der mathematischen physik. *Journal für die Reine und Angewandte Mathematik*, 135:1–61, 1909.

[29] C. C. J. Roothaan. New developments in molecular orbital theory. *Rev. Mod. Phys.*, 23:69–89, 1951.

[30] Marco Sarich, Frank Noé, and Christof Schütte. On the approximation error of markov state models. *SIAM Multiscale Model. Simul.*, 8:1154–1177, 2010.

[31] C. Schütte, A. Fischer, W. Huisinga, and P. Deuflhard. A Direct Approach to Conformational Dynamics based on Hybrid Monte Carlo. *J. Comput. Phys.*, 151:146–168, 1999.

[32] C. Schütte, F. Noé, J. Lu, M. Sarich, and E. Vanden-Eijnden. Markov state models based on milestoning. *J. Chem. Phys.*, 134:204105, 2011.

[33] Christof Schütte, Frank Noé, Eike Meerbach, Philipp Metzner, and Carsten Hartmann. Conformation Dynamics. In R. Jeltsch and G. Wanner (Eds), editors, *Proceedings of the International Congress on Industrial and Applied Mathematics (ICIAM)*, pages 297–336. EMS publishing house, 2009.

[34] David E. Shaw, Paul Maragakis, Kresten Lindorff-Larsen, Stefano Piana, Ron O. Dror, Michael P. Eastwood, Joseph A. Bank, John M. Jumper, John K. Salmon, Yibing Shan, and Willy Wriggers. Atomic-Level Characterization of the Structural Dynamics of Proteins. *Science*, 330(6002):341–346, October 2010.

[35] N. Singhal and V. S. Pande. Error analysis and efficient sampling in Markovian state models for molecular dynamics. *J. Chem. Phys.*, 123:204909, 2005.

[36] A. Spaar, C. Dammer, R. R. Gabdoulline, R. C. Wade, and V. Helms. Diffusional encounter of barnase and barstar. *Biophys J*, 90:1913–1924, 2006.

[37] W. C. Swope, J. W. Pitera, and F. Suits. Describing protein folding kinetics by molecular dynamics simulations: 1. Theory. *J. Phys. Chem. B*, 108:6571–6581, 2004.

[38] Attila Szabo and Seil S. Ostlund. *Modern quantum chemistry*. Dover Publications, Mineola, NY, 1982.

[39] N. G. van Kampen. *Stochastic Processes in Physics and Chemistry*. Elsevier, Amsterdam, 4th edition, 2006.

[40] Vincent A. Voelz, Gregory R. Bowman, Kyle Beauchamp, and Vijay S. Pande. Molecular Simulation of ab Initio Protein Folding for a Millisecond Folder NTL9. *J. Am. Chem. Soc.*, 132(5):1526–1528, February 2010.

[41] S. Meyn W. Huisinga and Ch. Schuette. Phase transitions and metastability for markovian and molecular systems. *Ann. Appl. Probab.*, 14:419458, 2004.

[42] D. J. Wales. *Energy Landscapes*. Cambridge University Press, Cambridge, 2003.

[43] D. J. Wales and J. P. K. Doye. Stationary points and dynamics in high-dimensional systems. *J. Chem. Phys.*, 119:12409–12416, 2003.

[44] Marcus Weber. *Meshless Methods in Conformation Dynamics*. PhD thesis, 2006.

Department of Mathematics and Research Center Matheon, FU Berlin, Arnimallee 6, 14195 Berlin, Germany

E-mail address: frank.noe@fu-berlin.de